Constraints of the 9-Methyl Group Binding Pocket of the Rhodopsin Chromophore Probed by 9-Halogeno Substitution†

Yajie Wang,‡ Petra H. M. Bovee-Geurts,§ Johan Lugtenburg,‡ and Willem J. DeGrip*,‡,§

Department of Bioorganic Photochemistry, Leiden Institute of Chemistry, Gorlaeus Laboratories, University of Leiden, Post Office Box 9502, 2300 RA Leiden, The Netherlands, and Department of Biochemistry UMC-160, Nijmegen Center for Molecular Life Sciences, University of Nijmegen Medical School, Post Office Box 9101, 6500 HB Nijmegen, The Netherlands

Received July 27, 2004; Revised Manuscript Received September 11, 2004

ABSTRACT: Sterical constraints of the 9-methyl-binding pocket of the rhodopsin chromophore are probed using retinal analogues carrying substituents of increasing size at the 9 position (H, F, Cl, Br, CH_3, and I). The corresponding 11-*Z* retinals were employed to investigate formation of photosensitive pigment, and the primary photoproduct was identified by Fourier transform infrared difference spectroscopy. In addition, any effects of cumulative strain were studied by introduction of the 9-*Z* configuration and/or the α-retinal ring structure.Our results show that the 9-F analogue still can escape from the 9-methyl-binding pocket and that its photochemistry behaves very similar to the 9-demethyl analogue. The 9-Cl and 9-Br analogues behave very similar to the native 9-methyl pigments, but the 9-I retinal does not fit very well and shows poor pigment formation. This puts an upper limit on the radial dimension of the 9-methyl pocket at 0.45−0.50 nm. Introduction of the α-retinal ring constraint in the 11-*Z* series results in cumulative strain, because the 9-I and 9-Br derivatives cannot bind to generate a photopigment. The 9-*Z* configuration can partially compensate for the additional α-retinal strain. The corresponding 9-Br analogue does form a photopigment, and the other derivatives give increased photopigment yields compared to the corresponding 11-*Z* derivatives. In fact, 9-*Z*-α-retinal would be an interesting candidate for retinal supplementation studies. Our data provide direct support for the concept that the 9-methyl group is an important determinant in ligand anchoring and activation of the protein and in general agree with a three-point interaction model involving the ring, 9-methyl group, and aldehyde function.

Rhodopsin is the photosensor of the rod photoreceptor cell in the vertebrate retina and consists of the protein opsin and a photosensitive ligand (chromophore, 11-*Z* retinal), linked via a protonated Schiff base (PSB)[1] to Lys296 of opsin. Photoexcitation of rhodopsin triggers a cascade of discrete, structurally and spectrally distinct, photointermediates. The light-dependent reaction, photoisomerization of the chromophore to the all-trans conformation, generates the first well-characterized photoproduct, bathorhodopsin (Batho). The subsequent dark reactions involve conformational rearrangements in both chromophore and protein to generate within milliseconds after illumination the active conformation, metarhodopsin II (Meta-II), which binds and activates the G-protein transducin (*1*−*3*). To date, the most detailed structural information on the chromophore of rhodopsin has been obtained by solid-state NMR (ssNMR), resonance Raman (RR), and Fourier transform infrared (FTIR) spectroscopy (*4*, *5*).

Studies with a large panel of retinal analogues have demonstrated that the opsin-binding site imposes specific sterical constraints upon the ligand conformation that can qualitatively explain why all-trans and 13-*Z* retinal do not fit into the binding site (*6*). ssNMR data are indicative of a smooth induced fit of the 11-*Z* chromophore in the rhodopsin-binding site, with the ring, 9-methyl group, and carbonyl group as major guiding elements for proper positoning (*7*). Such a three-point interaction model is also indicated by ssNMR studies on isorhodopsin, an artificial rhodopsin analogue generated by incorporating another retinal stereoisomer, 9-*Z* retinal, into the opsin-binding site. Here, the data suggest a strained ligand conformation encountering significant sterical interaction with the protein along the ring and 9-methyl group. Apparently, while a stable PSB can be formed, the binding site constraints do not allow the 9-*Z* configuration to induce an overall proper fit, a phenomenon we have dubbed an "induced misfit" (*8*).

FTIR difference spectroscopy of photointermediates in combination with site-directed mutagenesis and isotope labeling demonstrated that the majority of the peaks in the rhodopsin to Batho difference spectra reflect the isomerization of the chromophore, while the subsequent transitions

† Supported by a Grant from the Chemical Council of the Netherlands Organization for Scientific Research (NWO-CW, 700.98.013) to W.J.D. and J.L.

* To whom correspondence should be addressed. Fax: +31-243616413. Phone: +31-243614263. E-mail: wdegrip@baserv.uci.kun.nl.

‡ University of Leiden.

§ University of Nijmegen Medical School.

[1] Abbreviations: 9-H/F/Cl/Br/I-(α)-rhodopsin, opsin regenerated with 11-*Z* 9-H/F/Cl/Br/I-(α)-retinal; 9-H/F/Cl/Br/I-(α)-isorhodopsin, opsin regenerated with 9-*Z* 9-H/F/Cl/Br/I-(α)-retinal; 9-dm-rhodopsin, opsin regenerated with 11-*Z* 9-desmethyl retinal; Batho, bathorhodopsin; DoM, dodecyl-1-*β*-maltoside; FTIR, Fourier transform infrared; HOOP, hydrogen out-of-plane; Lumi, lumirhodopsin; Meta-I, metarhodopsin I; Meta-II, metarhodopsin II; PSB, protonated Schiff base; RR, resonance Raman; ssNMR, solid-state nuclear magnetic resonance.

10.1021/bi048404h CCC: $27.50
Published on Web 10/30/2004

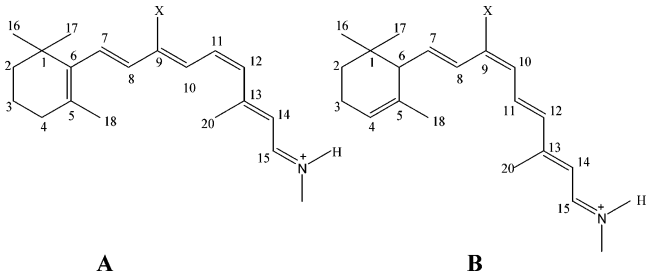

A **B**

FIGURE 1: Chemical structure and numbering of the 9-substituted retinals used in this study shown as the PSB present in the corresponding pigments. X = CH_3 (methyl), I, Br, Cl, F, H (demethyl). (A) 11-*Z* retinal derivatives (rhodopsin analogues). The corresponding isorhodopsin analogues have a 9-*Z* and an 11-*E* configuration instead. (B) 9-*Z* α-retinal derivatives (α-isorhodopsin analogues). The corresponding α-rhodopsin analogues have a 9-*E* and an 11-*Z* configuration instead.

present a gradual increase in protein activity (*4*, *9*, *10)*. The intense hydrogen out-of-plane (HOOP) vibrations in the rhodopsin to Batho FTIR difference spectra correlate with those observed in RR spectra of Batho and are regarded to reflect twisting around the single bonds in the all-trans chromophore constrained by steric ligand−protein interactions (*5*, *11*−*13*). Such torsional strain in the chromophore has been proposed as a potential mechanism to store part of the photon energy adsorbed by rhodopsin (*5*, *14*, *15*). The picture emerges that, at the Batho stage, close contacts between the isomerized ligand and opsin hold the former in a strained conformation and function as "transfer points" by which the torsional strain in the polyene chain is mediated to drive the conformational changes in the protein moiety. Potential candidates to mediate steric interactions between opsin and retinal are the protruding retinal side-chain methyl groups. Single demethyl analogues of rhodopsin (9- or 13-demethyl) have been examined before and show distinct effects on rhodopsin functionality (*5*, *10*, *11*, *16*−*21*). For instance, 11-*Z* 9-demethyl retinal does recombine to form a photosensitive pigment that however exhibits a strong blue shift in the main absorbance band (λ_{max} = 465 nm) compared to rhodopsin (λ_{max} = 498 nm) and a reduced potential to generate the active state Meta-II (*21*−*29*).

Here, we investigate the steric constraints of the 9-methyl-binding pocket of the chromophore-binding site in opsin using 9-halogeno 11-*Z* and 9-*Z* retinal and the corresponding α-retinal analogues, exploiting the broad size range covered by the van der Waals radii of halogen subsitutents (F ∼ 0.135 nm, Cl ∼ 0.180 nm, Br ∼ 0.195 nm, and I ∼ 0.215 nm, compared to H ∼ 0.120 nm and CH_3 ∼ 0.20 nm) (*30*).

MATERIALS AND METHODS

Synthesis of Retinal Derivatives. The chemical structure of the retinal derivatives used in this report is shown in Figure 1. The synthesis of the 9-substituted retinals and α-retinals was performed via a stereodominant procedure as described elsewhere (*31*, *32*). The 9-*Z* and 11-*Z* isomers were purified using silicagel column chromatography (eluent 3% diethyl ether in petroleumether). The purity of the compounds was verified using ^{1}H and ^{13}C NMR and mass spectrometry (*31*, *32*) and was always better than 99%. PSBs were prepared by addition of excess *N*-butylamine to a retinoid solution in hexane, evaporation of the solvent, dissolution of the resulting Schiff base in ca. 10 μL of methanol, followed by immediate addition of 1 mL of an acidified solution of 1% Triton X-100 (pH 2). Spectra were taken on a Perkin−Elmer lambda 18 double-beam spectrophotometer.

Generation of Analogue Pigments. Bovine rod outer segment membranes in the opsin form (opsin membranes) were prepared from fresh, light-adapted, eyes as described (*33*). The regeneration capacity of these preparations was estimated from the A_{500}/A_{280} ratio obtained upon subsequent incubation with a 3-fold excess of 11-*Z* retinal, whereby a ratio of 2.0 was taken to represent membranes with maximal rhodopsin content. Rhodopsin and analogue pigments were prepared from opsin membranes showing a regeneration capacity in the range of 90−100%. All manipulations were done under dim red light (>620 nm, Schott RG620 long-pass filter). Analogue pigments were generated by incubating opsin membranes for at least 3 h to overnight at room temperature with a 3−10-fold molar excess of retinal. Here, opsin membranes were suspended in buffer A (20 mM Pipes, 130 mM NaCl, 5 mM KCl, 2 mM $CaCl_2$, 0.1 mM EDTA, and 1 mM dithioerythreitol at pH 6.5), to a final concentration in opsin of 50 μM. The retinals were added in a small volume of dimethylformamide (≤4% final volume), and the incubation was performed in an inert argon atmosphere. Extent of pigment formation was assessed after incubation for 1 h as described below, and if this was <50% of the control (11-*Z* or 9-*Z* retinal), a second aliquot of the retinal analogue was added. This was repeated until the pigment formation had leveled. About 10-fold molar excess was used for the 9-iodo analogues. The level of unreacted opsin was finally estimated in a small aliquot from the extra amount of rhodopsin formed upon addition of 11-*Z* retinal. The total absorbance equivalent of pigment finally obtained in this sample ($\Delta A_{(pigment)}$ at $\lambda_{max(pigment)}$ + $\Delta A_{498(rhodopsin)}$) always was within 10% of the control value, indicating that the molar absorbance coefficients of the pigments will not deviate strongly from the control. To remove excess retinal, it was converted into the corresponding oxime by addition of hydroxylamine to a final concentration of 10 mM and subsequently largely (>90%) removed by two extractions with a 50 mM solution of heptakis (2,6-di-*O*-methyl)-β-cyclodextrin (Aldrich), which produces a soluble inclusion complex with retinals and retinaloximes (*34*, *35*), followed by washing twice with double-distilled water. To restore the native lipid/protein ratio, the resulting pigments were then dissolved in 20 mM nonyl-1-β-glucoside in buffer A and mixed with 50-fold molar excess of Asolectin (Sigma), a crude soybean lipid extract containing a mixture of several lipids. Reconstitution in proteoliposomes was accomplished by rapid dilution as described before (*36*). The resulting pigment membranes were finally washed with double-distilled water and stored at −80 °C until further use.

In the case of 11-*Z* 9-iodoretinal, yields of photopigment were low and required a large excess of retinal, the photopigment was quite unstable, and extraction with cyclodextrin was not very successful. Hence, we purified the pigment from excess oxime by ConA-Sepharose affinity chromatography as described (*33*) with nonyl-1-β-glucoside as the detergent. The purified pigment was reconstituted into retina lipid proteoliposomes by detergent dilution (*36*).

Spectral Properties of the Analogue Pigments. UV−visible spectra of pigment membranes suspended in buffer A to a final concentration of about 1 μM of pigment were recorded

on a Perkin−Elmer lambda 18 double-beam spectrophotometer equipped with an end-on photomultiplier detector. A circulating bath was used to control the sample temperature. The sample was bleached for 3 min (Schott OG470 long-pass filter for analogue pigments and Schott OG530 long-pass filter for rhodopsin). The wavelength of maximal absorbance (λ_{max}) of rhodopsin and the analogue pigments was determined from the peak position in the difference spectrum obtained by subtracting the spectrum after illumination from the dark state spectrum, both taken in the presence of 10 mM hydroxylamine in mixed micellar solution (20 mM DoM in buffer A).

FTIR Spectroscopy. FTIR analyses were performed on a Bruker IFS 66/S spectrometer equipped with a liquid nitrogen cooled, narrow band, HgCdTe (MCT) detector. Spectra were taken at 2 cm^{-1} resolution. The sample temperature was computer-controlled using a variable temperature helium-cooled cryostat (Heliostat, APD Cryogenics Inc.), which was evacuated and had a set of NaCl windows in the infrared light path. For analysis of the first photoproduct, the sample temperature was kept at 80.0 ± 0.2 K. Membrane films of the samples were prepared by isopotential spin-drying 1−2 nmol of pigment on an AgCl window (Crystran Limited, U.K.), which were then rehydrated with buffer A and sealed using a second AgCl window and a rubber O-ring spacer as described (*37*, *38*). Samples were illuminated in the spectrometer using a modified (150 W halogen) fiberoptics ringilluminator (Schott) equipped with a 488 ± 10 nm interference filter (Schott) and a set of long-pass filters. Typically six spectra (1280 scans each, at a 120 s acquisition time per spectrum) were taken and averaged of the dark-state receptor and, subsequently, following illumination for 300 s through the interference filter, of the photointermediate state. Difference spectra were calculated by subtracting these blocks of spectra. The Batho intermediates could be completely photoreversed by illuminating the sample for 300 s with light of 610 nm (Schott RG610 long-pass filter), as evidenced from the successive difference spectra.

RESULTS

Retinals Used in This Study. The retinal derivatives used in this study (Figure 1) were primarily designed to probe the sterical constraints of the 9-methyl-binding niche in the chromophore-binding site of rodopsin. For this purpose, a novel range of substituents was introduced at the 9 position (F, Cl, Br, and I) that with respect to their van der Waals radius bridge the gap between the 9-H (9-demethyl) derivative (which yields a functionally defective pigment) and the native 9-methyl derivative (yielding rhodopsin). Two other modifications were introduced to test any cumulative effects. Earlier, we demonstrated that a shift of the *Z* configuration from the 11═12 to the 9═10 bond impairs a smooth fit of the ligand in the binding site, and binding is accompanied with sterical strain in the ring and the 8−10 segment (*8*). Hence, we also prepared 9-*Z* retinal with the same set of 9-substituents to analyze the corresponding isorhodopsin analogues. Finally, it was reported that a shift of the ring double bond from the 5/6 to the 4/5 position (α-retinal) results in less efficient binding with significant lower kinetics of pigment formation for both the 11-*Z* and the 9-*Z* isomer, probably because the modified ring cannot make a proper fit with the ring-binding pocket (*39*). Consequently, we also introduced the set of 9-substituents in α-retinal in combination with the 11-*Z* as well as the 9-Z configuration.

Table 1: Spectral Properties of 11-*Z*-9-Halogeno Retinals and Corresponding Analogue Pigments

substituent (11-*Z*)	absorbance maximum[a] (nm)			opsin shift[b] (cm^{-1})	pigment formation[c]
	aldehyde	PSB	pigment		
9-methyl (native)	365	440	498	2650	≡100
9-iodo	353	414	484	3490	±
9-bromo	363	425	485	2910	+
9-chloro	345	415	485	3480	+
9-fluoro	348	420	466	2350	+
9-H (demethyl)	359	434	466	1580	++

[a] The aldehyde was measured in a hexane solution; the protonated Schiff base, in a 1% Triton X-100 solution (pH 2); and the pigment, in a 1% DoM solution (pH 6.5). Accuracy is ±2 nm. [b] The opsin shift is calculated as the energy difference between the main absorbance maximum of the free protonated retinylidene Schiff base and that of the corresponding pigment and hence reflects the extent of modulation of the electronic properties of the ligand by the protein. In view of the ±2 nm accuracy in the peak wavelengths, the error in the opsin shift is ±200 cm^{-1}. [c] ++, >80% of the pigment generated compared to 11-*Z* retinal; +, 50−70%; and ±, 20−40%. The molar absorbance coefficient of the analogue pigments is assumed to be similar to that of rhodopsin (see Materials and Methods).

Table 2: Spectral Properties of 9-*Z*-9-Halogeno Retinals and Corresponding Analogue Pigments

substituent (9-*Z*)	absorbance maximum[a] (nm)			opsin shift[b] (cm^{-1})	pigment formation[c]
	aldehyde	PSB	pigment		
9-methyl (native)	362	431	485	2580	++
9-iodo	368	425	482	2780	≈
9-bromo	352	422	474	2600	+
9-chloro	363	419	474	2770	+
9-fluoro	354	410	465	2880	+
9-H (demethyl)	361	431	465	1700	++

[a] The aldehyde was measured in a hexane solution; the protonated Schiff base, in a 1% Triton X-100 solution (pH 2); and the pigment, in a 1% DoM solution (pH 6.5). Accuracy is ±2 nm. [b] The opsin shift is calculated from the protonated SB and pigment data as outlined in the footnote of Table 1. [c] ++, >80% of the pigment generated compared to 9-*Z* retinal; +, 50−70%; and ≈, <20%. The molar absorbance coefficient of the analogue pigments is assumed to be similar to that of isorhodopsin (see the Materials and Methods). Pigment formation with 9-*Z* retinal (isorhodopsin) is comparable to that of 11-*Z* retinal (rhodopsin).

All retinals were prepared using newly developed stereodominant synthetic schemes that greatly facilitated the isolation of pure isomers (*31*, *32*). Peak wavelengths of the aldehydes in hexane and of the corresponding protonated *N*-retinylidene butyliminium chloride Schiff bases in 1% Triton X-100 solution are collected in Table 1 (11-*Z* isomers), Table 2 (9-*Z* isomers), and Table 3 (11-*Z* and 9-*Z* α-isomers). Data are only provided for retinoids that yielded detectable quantities of photosensitive pigment upon incubation with bovine opsin.

Rhodopsin Analogues. UV−vis difference spectra of the family of rhodopsin analogues generated with the 11-*Z* retinal derivatives are shown in Figure 2. Such spectra served to establish the peak wavelength of the obtained pigments. The retinaloxime derivatives produced upon illumination show a slight dependence of the peak wavelength on the 9-substituent. This is not at all reflected in the pigments, however, which point at differential effects of the protein

Table 3: Spectral Properties of 11-*Z*- and 9-*Z*-9-Halogeno α-retinals and Corresponding Analogue Pigments[a]

substituent (α-retinal)	absorbance maximum[b] (nm)			opsin shift[c] (cm^{-1})	pigment formation[d]
	aldehyde	PSB	pigment		
9-methyl 11-*Z*	352	424	469	2260	+
9-chloro 11-*Z*	346	408	454	2480	±
9-fluoro 11-*Z*	340	406	448	2310	+
9-H 11-*Z*	344	413	446	1790	++
9-methyl 9-*Z*	348	417	461	2290	++
9-bromo 9-*Z*	341	397	448	2870	±
9-chloro 9-*Z*	343	405	443	2120	±
9-fluoro 9-*Z*	337	399	437	2180	++
9-H 9-*Z*	342	411	444	1810	++

[a] The 9-iodo-α-retinals and the 11-Z 9-bromo-α-retinal did not generate detectable quantities of photosensitive pigment. [b] The aldehyde was measured in a hexane solution; the protonated Schiff base, in a 1% Triton X-100 solution (pH 2); and the pigment, in a 1% DoM solution (pH 6.5). Accuracy is ±2 nm. [c] The opsin shift is calculated from the protonated SB and pigment data as outlined in the footnote of Table 1. [d] ++, >70% of the pigment generated compared to the control (11-*Z* retinal); +, 50−70%; and ±, 20−40%. The molar absorbance coefficient of the analogue pigments is assumed to be similar to that of rhodopsin (see the Materials and Methods).

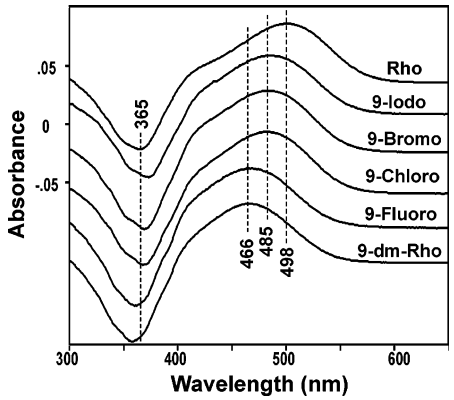

FIGURE 2: Pigment formation by 11-*Z*-9-X-retinal analogues assayed by UV−vis difference spectroscopy. Purified pigments were dissolved in 20 mM DoM in buffer A, and UV−vis spectra were taken before (1) and after (2) illumination in the presence of 10 mM hydroxylamine. Shown are the corresponding difference spectra (1−2), exhibiting the main pigment absorbance band as a positive peak and the retinaloxime band generated upon illumination as a negative peak. Note the different spectral shifts of the pigment and oxime peaks with respect to rhodopsin.

environment. The latter is even more evident in the opsin shift (Table 1), which is a measure for the impact of the protein environment on the electronic energy levels of the bound ligand. When a ca. 200 cm^{-1} inaccuracy in the opsin shift estimation is taken into account, this parameter is substantially larger in the 9-Cl and 9-I pigments (ca. 3500 cm^{-1}) and much smaller in the 9-demethyl rhodopsin (1580 cm^{-1}) than in rhodopsin itself (2650 cm^{-1}). A different distribution is apparent with respect to the wavelength of the peak absorbance. The 9-I, -Br, and -Cl pigments all exhibit a small 13−14 nm blue shift relative to rhodopsin, while the 9-F pigment shows the same large blue shift (32 nm) as 9-demethylrhodopsin.

Good to excellent pigment formation is observed for all 11-*Z* derivatives except 9-iodo. Even a large excess of 9-iodo 11-*Z* retinal only resulted in 20−25% pigment formation, and the thermal stability of the pigment proved to be much lower than that of the other family members. Removal of excess 9-I retinal by cyclodextrin extraction was inefficient and resulted in loss of pigment. The 9-I pigment could be purified more efficiently by lectin-affinity chromatography, but also then, the low thermal stability gave problems and the quality of the final preparation was suboptimal, as indicated by a relatively high A_{280}/A_{max} ratio of 3 (1.7 for rhodopsin under comparable conditions).

Isorhodopsin Analogues. The isorhodopsin analogues generated from the 9-*Z* retinal derivatives present a pattern interestingly different from the rhodopsin analogues (Table 2). The opsin shifts now are comparable for most family members and are in fact similar to that of rhodopsin, except for the 9-demethyl pigment that again presents a much lower opsin shift. Similar to their rhodopsin counterparts, the 9-demethyl and 9-F isorhodopsins also exhibit a large blue shift in the main absorbance band compared to isorhodopsin (20 nm) but almost no shift compared to the 9-demethyl and 9-F rhodopsins. The 9-Br and 9-Cl isorhodopsins behave similar to the corresponding rhodopsin derivatives (11 nm blue shift relative to isorhodopsin), but 9-I isorhodopsin deviates; it not only exhibits a very small blue shift relative to isorhodopsin (3 nm) but also relative to 9-I rhodopsin (2 nm).

Pigment formation with the 9-*Z* derivatives follows the 11-*Z* pattern: good to excellent except for the 9-I derivative that even produced less pigment (10−15%) than the corresponding 11-*Z* derivative (20−25%). Nevertheless, the 9-I isorhodopsin easily survived extraction of the excess retinal with cyclodextrin and is probably thermally more stable than the 9-I rhodopsin.

α-*Retinal-Based Analogue Pigments.* The additional constraint introduced by the different modes of freedom in the ring of the α-retinals clearly produces cumulative strain when combined with several larger substituents. Neither the 9-I and 9-Br 11-*Z* α-retinals nor the 9-I 9-*Z* α-retinal generated detectable amounts of photosensitive pigment. Overall, the 9-*Z* α-retinals were superior to the 11-*Z* α-retinals in pigment formation (Table 3).

The opsin shifts were also measured for all α-retinal-derived pigments. Now, the 9-methyl, 9-Cl, and 9-F analogues show similar opsin shifts (2120−2480 cm^{-1}) that are somewhat smaller than for rhodopsin (2650 cm^{-1}). Again, the opsin shift of the demethyl analogues was substantially smaller (∼1800 cm^{-1}). The 9-BR, 9-*Z* derivative exhibits an unusual large opsin shift (2870 cm^{-1}).

The wavelength of maximal absorbance shows a regular pattern. All α pigments exhibit a 20−30 nm blue shift respective to the corresponding normal pigments. Within the α series, the 9-*Z* pigments present a small blue shift (8−11 nm) relative to the corresponding 11-*Z* pigments, except for the 9-demethyl analogues that are very close. Within the 9-*Z* α series as well as the 11-*Z* α series, a gradual blue shift in the absorbance band is observed going from the methyl- to the fluoropigment. This is not paralleled in the corresponding aldehyde or PSBs.

Photoproduct Formation at 80 K Analyzed by FTIR. Because the rhodopsin to Batho difference spectra are dominated by changes in the vibrational state of the retinal chromophore as a result of isomerization and conformational strain, we expect that this transition will yield the most pronounced differences in the FTIR spectra of analogue pigments. Also, it has been reported that 9-demethyl-

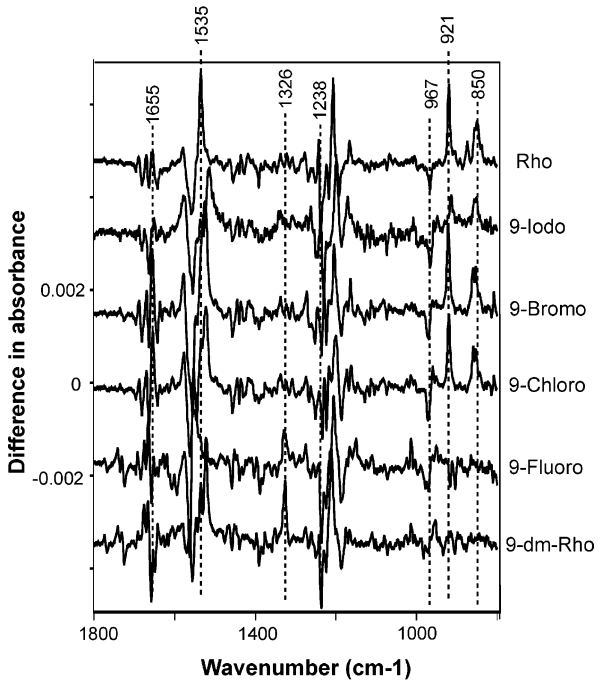

FIGURE 3: Photoproduct formation from 11-*Z*-9-X-retinal analogue pigments at 80 K assayed by FTIR difference spectroscopy. Purified pigments were deposited as membrane films on an AgCl window and FTIR spectra were taken at 80 K before (1) and after (2) illumination. Shown are the corresponding difference spectra (2−1), where negative peaks reflect vibrational bands of the pigment that change upon photoproduct formation and positive peaks represent newly arising vibrational absorbance bands of the photoproduct. Some characteristic vibrational bands are indicated to highlight changes in the analogue spectra.

rhodopsin already shows aberrant photochemical behavior at temperatures where the Batho product photogenerated from rhodopsin is still stable (<130 K) (*24*). Because rhodopsin and isorhodopsin produce the same Batho intermediate and the ring of the chromophore is not involved yet in the early transitions (*40*, Pistorius et al., unpublished), our FTIR analysis here focuses on the photoproduct formation of the 9-substituted rhodopsin analogues. The corresponding difference spectra are presented in Figure 3. Negative peaks (−) represent vibrational modes in the pigment that undergo a change upon transition to the photoproduct, while positive peaks (+) represent characteristic vibrational modes of the photoproduct. The overall pattern is very similar for the 9-methyl, 9-I, 9-Br, and 9-Cl analogues on one hand and for the 9-F and 9-demethyl analogues on the other hand.

The native rhodopsin to Batho difference spectrum is shown at the top of Figure 3. Most of the bands in this spectrum have been assigned to specific vibrations of the retinal backbone (C═C and C−C stretch vibrations around 1550 and 1200 cm^{-1}, respectively) and HOOP vibrations, absorbing below 1000 cm^{-1} (*5*, *13*, *41*, *42*). The small yet very characteristic changes in the amide I region (1700−1630 cm^{-1}) represent subtle conformational changes in the protein moiety. The bands at 1558 cm^{-1} (−) and 1535 cm^{-1} (+) in the rhodopsin to Batho difference spectrum have been assigned to the C_7═C_8 and the C_{11}═C_{12} stretching modes (*13*). Characteristic vibrational modes of the chromophore are found in the C−C stretch region (1150−1250 cm^{-1}), appropriately indicated as the "fingerprint region". Bands at 1244 (+) and 1238 (−) cm^{-1} (C_{12}−C_{13} stretch), 1220 (+) and 1214 (−) cm^{-1} (C_8−C_9 stretch), 1210 (+) and 1190 (−) cm^{-1} (C_{14}−C_{15} stretch), and 1166 (+) cm^{-1} (C_{10}−C_{11} stretch) have already been assigned (*41*) and reflect the 11-*Z* to all-*E* isomerization of the chromophore. In these three regions (amide I, C═C stretch, and fingerprint), subtle changes are apparent in the 9-analogue pigments, which will be discussed below. Most pronounced differences are found in the HOOP region (1000−700 cm^{-1}). The 969 (−) cm^{-1} band of rhodopsin has been assigned to the strongly coupled C_{11}H and C_{12}H wags ($HC_{11}dC_{12}H$ A2 HOOP), indicative of torsion in the C_{10}−C_{13} region (*12*, *42*). The positive vibrational modes at 921, 875, and the triplet near 850 cm^{-1} are very characteristic of Batho and have been shown to contain contributions of the C_{14}H (848 cm^{-1}), C_{10}H (875 cm^{-1}), and HC_7dC_8H B*g* (838 cm^{-1}) wags and the (uncoupled) C_{11}H (921 cm^{-1}) and C_{12}H (858 cm^{-1}) wags (*13*). The intensity of these Batho modes reflect strong conformational perturbation of the all-*E* chromophore structure by constraints of the protein environment (*5*). These modes are largely maintained in the 80 K photoproduct of the 9-I, 9-Br, and 9-Cl analogues but are completely lacking in that of the 9-F and 9-demethyl analogues. The logical conclusion is that the former three analogue pigments initiate a normal photolytic pathway at 80 K to a stable Batho intermediate. This however is not the case for the 9-F and 9-demethyl pigments, which will be discussed in more detail below. We investigated whether a stable Batho intermediate could be generated for the latter two analogue pigments at lower temperatures, but difference spectra obtained as low as 10 K were still very similar to those shown in Figure 3.

DISCUSSION

Probe Selection. Several lines of evidence indicate that the ring and the 9-methyl group are important chromophore determinants in opsin−ligand interaction, not only contributing to proper chromophore anchoring in the active site but also to subsequent photoactivation of the protein (*3*, *6*, *7*, *16*, *28*, *40*). In addition, the 9-*Z* configuration will put strain on this anchoring mechanism (*8*). To probe the sterical constraints of the 9-methyl-binding pocket and potential cumulative effects of the presence of the 9-*Z* configuration and/or a different ring conformation, the retinoids shown in Figure 1 were prepared.

Several of the retinal analogues that we include here in our study have been described and analyzed for pigment formation before. The results that we present in Tables 1−3 for these compounds (11-*Z* and 9-*Z* 9-demethylretinal, 11-Z and 9-*Z* 9-methyl α-retinal, and 9-*Z* 9-F and 9-Br retinal) agree with earlier reports (*22*−*24*, *39*, *43*−*45*). We present fully novel data for all 9-halogeno derivatives and for the 9-demethyl α-retinals. The effect of the substituents on the spectral properties of the retinoids is a complex combination of electronegative, polarizing, and sterical properties and will not be discussed here.

Pigment Formation. In estimating pigment formation, we assumed that the molar absorbance coefficients of all pigments formed are within 10% of that of rhodopsin, based on earlier estimates for 9-demethylrhodopsin, 9-demethylisorhodopsin (*23*, *29*), and α-(iso)rhodopsins (*39*). In an independent check, we estimated the percentage of unreacted opsin by subsequent incubation with 11-*Z* retinal. The total

amount of pigment formed in absorbance units always was within 10% of that of the control (only 11-*Z* retinal). In fact, deviations in individual molar absorbance coefficients up to 25% will not change the general pattern of pigment formation presented in Tables 1−3.

The phenomenon of only partial pigment formation is quite common in rhodopsin analogue studies (for a review, see refs *23*, *46*, and *47*) and is often taken as an indication for binding site fitness. We think that other factors may have to be taken into consideration as well. Usually, it has not been assessed whether remaining opsin is still functional (e.g., can bind its native ligand). We have systematically checked this for all retinal analogues in this study and, as mentioned above, in case of partial pigment formation (+, ±, and ≈), we always find functional opsin remaining after analogue pigment formation has leveled and in quantities roughly equivalent to that expected based on the extent of analogue pigment production. Hence, despite the excess of analogue ligand present, the remaining functional opsin does not generate analogue pigment. This cannot be explained in terms of binding affinities and dynamic equilibrium distribution, because then addition of the high-affinity ligand 11-*Z* retinal would compete the analogue ligand away, and we do not observe a loss of analogue pigment. Another explanation might be envisioned if opsin is organized in functional oligomers with cooperative behavior (*48*). In that case, suboptimal occupation of the active site with a retinal analogue might lead to cooperative conformational changes resulting in restricted access in neighboring opsins only allowing the native ligand to enter. However, this explanation cannot account for our and others' observation that in detergent solution, where oligomer formation does not seem to occur, only partial analogue pigment formation is also commonly observed. Recently, evidence for the presence in opsin of secondary binding sites for retinoids was presented (*49*, *50*), an entrance site, the first stage on the way to the active site and only accessible when the active site is not occupied, and an exit site, only accessible from the active site after photoisomerization of the chromophore. The transition of the ligand from the entrance site to the active site would be rate-determining for pigment formation. Such a mechanism might explain partial pigment formation if an analogue ligand would become "stuck" in the entrance site to block access to the active site, and this block can only be relieved by a high-affinity ligand. A possible mechanism would be, considering that the entrance site may accommodate two retinoids (*50*), that in case of retinal analogues, which transfer only slowly to the active site, occupation of the entrance site with two analogue compounds may induce a slow conformational alteration in the entrance site, blocking access to the active site. Because the retinals in the entrance site are still in dynamic equilibrium with "bulk retinal", a high-affinity ligand, even added at equimolar quantity, will eventually compete the analogues away from the entrance site, reverse the inhibitory change, and be allowed access to the active site again. From this point of view, the extent of pigment formation will depend on several factors: the transfer rate of the ligand from the entrance site to the active site, the affinity of the ligand for the entrance site, and the rate with which double occupation of the entrance site will trigger the change to a nonaccess conformation. Because only the transfer rate will depend on the fit of the ligand within the active site, pigment formation will only reflect the latter parameter at low excess of analogue ligand where double occupancy of the entrance site is unlikely. To verify this hypothesis, detailed kinetic studies need to be performed.

It can be argued that the opsin shift is also a measure for the active-site fit of the ligand, because only an optimal fit will fully profit from the inductive effect of the protein environment. On the other hand, it should be taken into account that the opsin shift is a complex combination of the electronic properties of the ligand and the inductive potential of the protein. Our data, comprising a large group of closely related ligands, show some general trends. The opsin shifts of the four demethyl pigments measured are comparable and much smaller than that of all other pigments. In the remaining population, the 11-*Z* pigments (rhodopsins) generally exhibit a larger opsin shift than the 9-*Z* pigments (isorhodopsins), while the 11-*Z* α-retinal pigments (α-rhodopsins) exhibit the smallest opsin shift. Furthermore, in the subpopulations, the opsin shift is quite similar within the isorhodopsins and within the α-rhodopsins, but within the rhodopsins, the 9-I and 9-Cl analogues present unusually large opsin shifts. This is partly due to the relatively blue-shifted absorbance maxima of the corresponding PSBs. In the relatively unperturbed 9-*Z* configuration, the 9-substituted derivatives show a gradual blue shift in PSB absorbance going from 9-methyl to 9-F. This is most easily explained by stabilization of the ground state under the pertaining conditions through further delocalization of the positive charge under influence of the electronegative potential of the substituents that increases in the direction of $CH_3 \rightarrow F$. The remarkable behavior of the 9-I and 9-Cl PSBs in the 11-*Z* series therefore may reflect preferential stabilization of a different conformation. For instance, free 11-*Z* retinal exists in a dynamic equilibrium of the 12-s-*Z* and 12-s-*E* conformation, while the active site of opsin only allows the 12-s-*E* shape.

The overall picture arising from the data in Tables 1−3 is that the 11-*Z* configuration allows a better fit in the active site of opsin for the normal retinal derivatives (*β*-retinals), while the opposite is true for the α-retinals. In addition, there is a cumulative effect of steric hindrance at the ring and 9-methyl sites on the potential of a retinoid to fit within the active site.

Initial Photoproduct. It is obvious from Figure 3 that the effect of 9 substitution on most C−C stretch vibrations (1250−1150 cm^{-1} region) is negligible except for the C_8−C_9 vibration (1214 (−) and 1220 (+) cm^{-1} in rhodopsin and Batho, respectively), where the extra mass of the 9-substituent results in an increasing reduction in frequency going from 9-demethyl to 9-iodo. Clear effects are also observed for the C=C vibrational modes of the photoproducts (1535 (+) cm^{-1} in Batho). Here, a downshift of the vibrational frequency also reflects a more delocalized electronic structure of the polyene chain.

The overall pattern of the difference spectra in Figure 3, in combination with the presence of characteristic Batho HOOP modes only in the 9-Cl, 9-Br, and 9-I analogues, demonstrates that the latter pigments follow the normal pattern and upon photoactivation generate a Batho intermediate, which is stable at 80 K. Some of the HOOP modes are affected by 9 substitution. The C_{10} wag (875 (+) cm^{-1} in Batho) is not visible in the analogues and is probably strongly shifted down in frequency. In the 9-I Batho intermediate even

the C_{11} wag (921 (+) cm^{-1} in Batho) is somewhat downshifted. The intensity of the HOOP modes in the 9-I Batho is significantly reduced, which may indicate a somewhat less strained conformation of the all-*E* 9-I chromophore. The amide I peaks (1700−1600 cm^{-1} region) are more intense in the 9-Cl and 9-Br pigments compared to rhodopsin, in particularly, the 1655 cm^{-1} mode, which is typical for α-helical structure. It suggests that Batho formation in these two analogue pigments is accompanied with slightly more extended stretching of an α-helical segment. In the 9-I pigment, another pattern is apparent, where an α-helical segment seems to convert into a less well-ordered α-helical structure in the Batho intermediate.

The lack of Batho formation in the 9-demethyl and 9-F pigments is not due to a lower thermal stability, because also at 10 K, no trace of Batho HOOP modes is observed. Rather, as reported before for the 9-demethyl pigment (*24*), the spectra of these photoproducts resemble that of the next intermediate lumirhodopsin (Lumi), which normally is only observed at a temperature over 130 K (not shown). Apparently, the volume of a fluoro substituent does not suffice to constrain the protein in a Batho-like conformation.

Active-Site Constraints. With respect to active-site constraints, two global observations are important: first, the 9-halogeno derivatives within one family show a similar pattern (opsin shift at least comparable to the 9-methyl pigments, with pigment formation less than 70%), while the 9-demethyl derivatives consistently deviate (significantly smaller opsin shifts, with pigment formation > 80%); second, while the 9-*Z* α-retinals are more successful in pigment formation than the corresponding 11-*Z* α-retinals, both 9-I derivatives fail to generate a photopigment. We offer the following concept for explanation: all 9-halogeno substituents position into the 9-methyl-binding pocket in the ground state of the pigment. This would explain the large opsin shifts (optimal position for modulation by the protein) and suboptimal pigment formation (correct positioning of the electronegative substituent slows down active-site occupation). Upon photoisomerization, the 9-I, 9-Br, and 9-Cl substituents are able to constrain the protein in a Batho-like conformation in a way similar to that of the methyl group, at the same time trapping the chromophore in a torsionally strained all-*E* conformation. This most likely involves the 9-methyl-binding pocket. However, the 9-F substituent is too small to stabilize this sterically highly constrained active-site structure. It can escape from the 9-methyl-binding pocket and then follows a pathway similar to the 9-demethyl pigment. The much smaller opsin shift, rapid rate, and high extent of pigment formation of the 9-demethyl analogues is consistent with rapid occupation of the active site with suboptimal positioning for modulation by the protein environment.

The global pattern obtained with the 9-I derivatives indicates that the iodo substituent can hardly be fitted into the 9-methyl-binding pocket. This would explain the low pigment yield and low pigment stability in the 11-*Z* configuration and the even lower pigment yield in combination with other sterical constraints (9-*Z* configuration and/or α-retinal ring). This would put an upper limit on the radial restriction of this pocket in the order of 0.45−0.50 nm. This is remarkably well in line with the latest crystal structure (*51*), which puts the 9-methyl group radially surrounded by 5 side chains with the OH of Tyr268, C_2 of Thr118, one H of Gly188, the S of Met207, and C_3 and C_4 of Ile189, all at a center−center distance between 0.4 and 0.5 nm. Longitudinally, this pocket seems to be less restricted, because elongated flexible-rod-shaped substituents at the 9-position (ethyl, *n*-propyl, and *n*-butyl) can still be accommodated (*47*). The radial restriction can explain why more bulky less flexible substituents such as the phenyl or isopropyl group are not or hardly able to generate a photopigment (*47*, Wang et al., unpublished).

Our results provide support for a more strained chromophore in the 9-*Z* configuration with strong sterical contacts at the 9-methyl site (*8*). This is in line with our observation that combining the sterically controversial 9-iodo substituent with the 9-*Z* configuration leads to an even slower rate and lower extent of pigment formation than in the 11-*Z* configuration. A combination with another sterical constraint, the α ring, shows cumulative effects as well. The 9-I and 9-Br 11-*Z* α-retinals are not able to generate a photopigment, while the other 9-substituted 11-*Z* α-retinals are considerably less effective in photopigment formation than the corresponding normal retinals. Strikingly, in the α-retinal series, the 9-*Z* derivatives perform markedly better than the 11-*Z* derivatives. Apparently, the poor fit in the active site of 11-*Z* retinals with both a large substituent at the 9 position and a modified ring structure can be improved by changing into a 9-*Z* configuration. This would make 9-*Z* α-retinals interesting alternatives for retinal supplementation studies, for instance in retina degenerative diseases (*52*, *53*), because they can be chemically and metabolically distinguished from endogenous retinals and their photopigments are easily recognized because of the large blue shift in absorbance maximum.

Collectively our data emphasize the finely tuned contribution of ring and 9 substituent in recognition and correct positioning of the ligand in rhodopsin. This complements ssNMR studies indicating highly specific constraints for the ring and 9-methyl group in the active site (*7*, *8*, *40*, *54*). Ligand binding in opsin apparently follows an induced-fit three-point interaction model, with the ring, 9-methyl group, and aldehyde group as the determining selection elements.

CONCLUSIONS AND PROSPECTS

Together with previous studies on rhodopsins containing a 9-demethyl 11-*Z*-retinal analogue, this work provides a consistent picture on the conformational freedom of retinal in the active site of opsin. As reported before (*24*), the 9-demethyl pigment exhibits a fully disturbed photocascade, in which a clear Batho intermediate cannot be detected. Our results show that the 9-F analogue can still escape from the 9-methyl-binding pocket and its photochemistry behaves very similar to the 9-demethyl analogue, while the 9-I retinal does not fit very well and combines low affinity for opsin with a low thermal stability of the corresponding pigment. This puts an upper limit on the radial dimension of the 9-methyl pocket of 0.45−0.50 nm. The 9-Cl and 9-Br analogues may induce subtle structural differences in the Batho intermediate but overall behave very similar to the native 9-methyl pigments. Our data support the three-point interaction model and further emphasize the importance of finely tuned ligand−protein interactions in ligand selection and photoactivation of rhodopsin.

The 9-methyl group seems to be an important factor for the correct positioning of the retinal in the active site of opsin.

Moreover, the 9-methyl group seems to provide the necessary fixation of parts of the chromophore, which upon photoisomerization, constrain the protein in the Batho conformation and give rise to the torsional strain in the chromophore. This clearly deviates from the situation in cone pigments, where the 9-methyl group appears to have a less prominent function (*55*).

Two constraining elements can apparently mutually compensate. The 9-*Z* α-retinals are much superior to the corresponding 11-*Z* derivatives in pigment formation, and 9-*Z* 9-methyl α-retinal would actually be an interesting candidate for retinal supplementation studies.

The current picture is that the photon energy is stored as torsional strain in the chromophore at the Batho stage (*4*, *5*, *13*, *56*) and that the energy released upon relaxation of the strain is used to drive the protein conformational changes in the photocascade dark reaction. This is consistent with our observation that as long as the HOOP signals prevail, only very small changes in the amide I region are observed in the FTIR difference spectra of the primary photoproduct.

On the basis of their primary photoproduct, our prognosis is that 9-F rhodopsin will perform poorly in Meta II formation and activation of the G protein transducin at physiological pH, similar to 9-demethylrhodopsin (*24*−*29*), and that the other 9-halogeno pigments will have activities similar to rhodopsin. However, considering the varying electronegative potentials of these substituents, effects on the pK_a of the Schiff base and consequently on that of the Meta I ↔ Meta II equilibrium and on Meta III formation can be expected, and possibly on the pH profile of transducin activation as well. Such studies are in progress.

REFERENCES

1. Emeis, D., Kühn, H., Reichert, J., and Hofmann, K. P. (1982) Complex formation between metarhodopsin II and GTP-binding protein in bovine photoreceptor membranes leads to a shift of the photoproduct equilibrium, *FEBS Lett. 143*, 29−34.
2. Kibelbek, J., Mitchell, D. C., Beach, J. M., and Litman, B. J. (1991) Functional equivalence of metarhodopsin II and the G_t-activating form of photolyzed bovine rhodopsin, *Biochemistry 30*, 6761−6768.
3. Hofmann, K. P. (2000) Late photoproducts and signaling states of bovine rhodopsin, in *Molecular Mechanisms in Visual Transduction* (Stavenga, D. G., DeGrip, W. J., and Pugh, E. N., Jr., Eds.) pp 91−142, Elsevier Science Pub., Amsterdam, The Netherlands.
4. DeGrip, W. J., and Rothschild, K. J. (2000) Structure and mechanism of vertebrate visual pigments, in *Molecular Mechanisms in Visual Transduction* (Stavenga, D. G., DeGrip, W. J., and Pugh, E. N., Jr., Eds.) pp 1−54, Elsevier Science Pub., Amsterdam, The Netherlands.
5. Mathies, R. A., and Lugtenburg, J. (2000) The primary photoreaction of rhodopsin, in *Molecular Mechanisms in Visual Transduction* (Stavenga, D. G., DeGrip, W. J., and Pugh, E. N., Jr., Eds.) pp 55−90, Elsevier Science Pub., Amsterdam, The Netherlands.
6. Mirzadegan, T., and Liu, R. S. H. (1991) Probing the visual pigment rhodopsin and its analogs by molecular modeling analysis and computer graphics, *Prog. Retinal Eye Res. 11*, 57−74.
7. Creemers, A. F. L., Kiihne, S., Bovee-Geurts, P. H. M., DeGrip, W. J., Lugtenburg, J., and DeGroot, H. J. M. (2002) ^{1}H and ^{13}C MAS NMR evidence for pronounced ligand−protein interactions involving the ionone ring of the retinylidene chromophore in rhodopsin, *Proc. Natl. Acad. Sci. U.S.A. 99*, 9101−9106.
8. Creemers, A. F. L., Bovee-Geurts, P. H. M., DeGrip, W. J., Lugtenburg, J., and DeGroot, H. J. M. (2004) MAS NMR analysis of protein−chromophore interactions reveals an induced misfit in isorhodopsin, *Biochemistry*, in press.
9. DeGrip, W. J., Gray, D., Gillespie, J., Bovee-Geurts, P. H. M., VanDenBerg, E. M. M., Lugtenburg, J., and Rothschild, K. J. (1988) Photoexcitation of rhodopsin: Conformation changes in the chromophore, protein, and associated lipid, as determined by FTIR difference spectroscopy, *Photochem. Photobiol. 48*, 497−504.
10. Siebert, F. (1995) Application of FTIR spectroscopy to the investigation of dark structures and photoreactions of visual pigments, *Isr. J. Chem. 35*, 309−323.
11. Eyring, G., Curry, B., Mathies, R. A., Fransen, R., Palings, I., and Lugtenburg, J. (1980) Interpretation of the resonance Raman spectrum of bathorhodopsin based on visual pigment analogues, *Biochemistry 19*, 2410−2418.
12. Eyring, G., Curry, B., Broek, A., Lugtenburg, J., and Mathies, R. A. (1982) Assignment and interpretation of hydrogen out-of-plane vibrations in the resonance Raman spectra of rhodopsin and bathorhodopsin, *Biochemistry 21*, 384−393.
13. Palings, I., VanDenBerg, E. M. M., Lugtenburg, J., and Mathies, R. A. (1989) Complete assignment of the hydrogen out-of-plane wagging vibrations of bathorhodopsin: Chromophore structure and energy storage in the primary photoproduct of vision, *Biochemistry 28*, 1498−1507.
14. Warshel, A., and Barboy, N. (1982) Energy storage and reaction pathways in the first step of the vision process, *J. Am. Chem. Soc. 104*, 1469−1476.
15. Birge, R. R., Einterz, C. M., Knapp, H. M., and Murray, L. P. (1988) The nature of the primary photochemical events in rhodopsin and isorhodopsin, *Biophys. J. 53*, 367−385.
16. Corson, D. W., and Crouch, R. K. (1996) Physiological activity of retinoids in natural and artificial visual pigments, *Photochem. Photobiol. 63*, 595−600.
17. Kochendoerfer, G. G., Verdegem, P. J. E., VanDerHoef, I., Lugtenburg, J., and Mathies, R. A. (1996) Retinal analog study of the role of steric interactions in the excited-state isomerization dynamics of rhodopsin, *Biochemistry 35*, 16230−16240.
18. Wang, Q., Kochendoerfer, G. G., Schoenlein, R. W., Verdegem, P. J. E., Lugtenburg, J., Mathies, R. A., and Shank, C. V. (1996) Femtosecond spectroscopy of a 13-demethylrhodopsin visual pigment analogue: The role of non-bonded interactions in the isomerization process, *J. Phys. Chem. B 100*, 17388−17394.
19. Lou, J. H., Tan, Q., Karnaukhova, E. N., Berova, N., Nakanishi, K., and Crouch, R. K. (2000) Synthetic retinals: Convenient probes of rhodopsin and visual transduction process, *Methods Enzymol. 315*, 219−237.
20. Pan, D. H., Ganim, Z., Kim, J. E., Verhoeven, M. A., Lugtenburg, J., and Mathies, R. A. (2002) Time-resolved resonance Raman analysis of chromophore structural changes in the formation and decay of rhodopsin's BSI intermediate, *J. Am. Chem. Soc. 124*, 4857−4864.
21. Fritze, O., Filipek, S., Kuksa, V., Palczewski, K., Hofmann, K. P., and Ernst, O. P. (2003) Role of the conserved NPxxY(x)$_{5,6}$F motif in the rhodopsin ground state and during activation, *Proc. Natl. Acad. Sci. U.S.A. 100*, 2290−2295.
22. Blatz, P. E., Lin, M., Balasubramaniyan, P., Balasubramaniyan, V., and Dewhurst, P. B. (1969) A new series of synthetic visual pigments from cattle opsin and homologs of retinal, *J. Am. Chem. Soc. 91*, 5930−5931.
23. Kropf, A., Whittenberger, B. P., Goff, S. P., and Waggoner, A. S. (1973) The spectral properties of some visual pigment analogs, *Exp. Eye Res. 17*, 591−606.
24. Ganter, U. M., Schmid, E. D., Perez-Sala, D., Rando, R. R., and Siebert, F. (1989) Removal of the 9-methyl group of retinal inhibits signal transduction in the visual process. A Fourier transform infrared and biochemical investigation, *Biochemistry 28*, 5954−5962.
25. Corson, D. W., Cornwall, M. C., MacNichol, E. F., Jr., Tsang, S. H., Derguini, F., Crouch, R. K., and Nakanishi, K. (1994) Relief of opsin desensitization and prolonged excitation of rod photoreceptors by 9-desmethylretinal, *Proc. Natl. Acad. Sci. U.S.A. 91*, 6958−6962.
26. Morrison, D. F., Ting, T. D., Vallury, V., Ho, Y.-K., Crouch, R. K., Corson, D. W., Mangini, N. J., and Pepperberg, D. R. (1995) Reduced light-dependent phosphorylation of an analog visual pigment containing 9-demethylretinal as its chromophore, *J. Biol. Chem. 270*, 6718−6721.
27. Han, M., Groesbeek, M., Smith, S. O., and Sakmar, T. P. (1998) Role of the C_9 methyl group in rhodopsin activation: Characterization of mutant opsins with the artificial chromophore 11-*cis*-9-demethylretinal, *Biochemistry 37*, 538−545.

28. Meyer, C. K., Böhme, M., Ockenfels, A., Gärtner, W., Hofmann, K. P., and Ernst, O. P. (2000) Signaling states of rhodopsin—Retinal provides a scaffold for activating proton-transfer switches, *J. Biol. Chem. 275*, 19713−19718.
29. Vogel, R., Fan, G.-B., Sheves, M., and Siebert, F. (2000) The molecular origin of the inhibition of transducin activation in rhodopsin lacking the 9-methyl group of the retinal chromophore: A UV−vis and FTIR spectroscopic study, *Biochemistry 39*, 8895−8908.
30. Wagnière, G. H. (1973) General and theoretical aspects of the carbon−halogen bond, in *The Chemistry of the Carbon Halogen Bond* (Patai, S., Ed.) part I, pp 1−47, John Wiley and Sons, London, U.K.
31. Wang, Y.-J., Woo, W. S., VanDerHoef, I., and Lugtenburg, J. (2004) 9-Demethyl-9-haloretinals by Wadsworth−Emmons coupling—Easy preparation of pure (all-*E*), (9*Z*), and (11*Z*) isomers, *Eur. J. Org. Chem.* 2166−2175.
32. Wang, Y.-J., and Lugtenburg, J. (2004) 4,5-Didehydro-9-demethyl-9-halo-5,6-dihydroretinals and their 9-cyclopropyl and 9-isopropyl derivatives—Simple preparation of α-ionone derivatives and pure (all-*E*)-, (9-*Z*)-, and (11-*Z*)-α-retinals, *Eur. J. Org. Chem.* 3497−3510.
33. DeGrip, W. J., VanOostrum, J., Bovee-Geurts, P. H. M., VanDerSteen, R., VanAmsterdam, L. J. P., Groesbeek, M., and Lugtenburg, J. (1990) 10,20-Methanorhodopsins: (7*E*,9*E*,13*E*)-10,20-methanorhodopsin and (7*E*,9*Z*,13*Z*)-10,20-methanorhodopsin—11-*cis*-Locked rhodopsin analog pigments with unusual thermal and photo-stability, *Eur. J. Biochem. 191*, 211−220.
34. DeLange, F., Bovee-Geurts, P. H. M., VanOostrum, J., Portier, M. D., Verdegem, P. J. E., Lugtenburg, J., and DeGrip, W. J. (1998) An additional methyl group at the 10-position of retinal dramatically slows down the kinetics of the rhodopsin photocascade, *Biochemistry 37*, 1411−1420.
35. DeGrip, W. J., VanOostrum, J., and Bovee-Geurts, P. H. M. (1998) Selective detergent-extraction from mixed detergent/lipid/protein micelles, using cyclodextrin inclusion compounds: A novel generic approach for the preparation of proteoliposomes, *Biochem. J. 330*, 667−674.
36. DeGrip, W. J., Olive, J., and Bovee-Geurts, P. H. M. (1983) Reversible modulation of rhodopsin photolysis in pure phosphatidylserine membranes, *Biochim. Biophys. Acta 734*, 168−179.
37. Clark, N. A., Rothschild, K. J., Simon, B. A., and Luippold, D. A. (1980) Surface induced orientation of multilayer membrane arrays: Theoretical analysis and a new method with application to purple membrane fragments, *Biophys. J. 31*, 65−96.
38. DeLange, F., Merkx, M., Bovee-Geurts, P. H. M., Pistorius, A. M. A., and DeGrip, W. J. (1997) Modulation of the metarhodopsin I/metarhodopsin II equilibrium of bovine rhodopsin by ionic strength—Evidence for a surface charge effect, *Eur. J. Biochem. 243*, 174−180.
39. Asato, A. E., Zhang, B.-W., Denny, M., Mirzadegan, T., Seff, K., and Liu, R. S. H. (1989) A study of the binding site requirements of rhodopsin using isomers of α-retinal and 5-substituted α-retinal analogs, *Bioorg. Chem. 17*, 410−421.
40. Spooner, P. J. R., Sharples, J. M., Goodall, S. C., Seedorf, H., Verhoeven, M. A., Lugtenburg, J., Bovee-Geurts, P. H. M., DeGrip, W. J., and Watts, A. (2003) Conformational similarities in the β-ionone ring region of the rhodopsin chromophore in its ground state and after photoactivation to the metarhodopsin-I intermediate, *Biochemistry 42*, 13371−13378.
41. Palings, I., Pardoen, J. A., VanDenBerg, E. M. M., Winkel, C., Lugtenburg, J., and Mathies, R. A. (1987) Assignment of fingerprint vibrations in the resonance Raman spectra of rhodopsin, isorhodopsin, and bathorhodopsin: Implications for chromophore structure and environment, *Biochemistry 26*, 2544−2556.
42. Mathies, R. A., Smith, S. O., and Palings, I. (1987) Determination of retinal chromophore structure in rhodopsins, in *Resonance Raman Spectra of Polyenes and Aromatics* (Spiro, T. G., Ed.) pp 59−108, John Wiley and Sons, New York.
43. Okada, T., Kandori, H., Shichida, Y., Yoshizawa, T., Denny, M., Zhang, B.-W., Asato, A. E., and Liu, R. S. H. (1991) Spectroscopic study of the batho-to-lumi transition during the photobleaching of rhodopsin using ring-modified retinal analogues, *Biochemistry 30*, 4796−4802.
44. Colmenares, L. U., Zou, X.-L., Liu, J., Asato, A. E., Liu, R. S. H., DeLera, A. R., and Alvarez, R. A. (1999) 11,12-Difluororhodopsin and related odd-numbered fluororhodopsins. The use of $J_{F,F}$ for following a *cis*−*trans* isomerization process, *J. Am. Chem. Soc. 121*, 5803−5804.
45. Derguini, F., and Nakanishi, K. (1986) Synthetic rhodopsin analogs, *Photobiochem. Photobiophys. 13*, 259−283.
46. Balogh-Nair, V., and Nakanishi, K. (1982) The stereochemistry of vision, in *Stereochemistry* (Tamm, T., Ed.) pp 283−334, Elsevier Biomedical Press, Amsterdam, The Netherlands.
47. Liu, R. S. H., and Asato, A. E. (1990) The binding site of opsin based on analog studies with isomeric, fluorinated, alkylated, and other modified retinals, in *Chemistry and Biology of Synthetic Retinoids* (Dawson, M. I., and Okamura, W. H., Eds.) pp 52−75, CRC Press, Boca Raton, FL.
48. Liang, Y., Fotiadis, D., Filipek, S., Saperstein, D. A., Palczewski, K., and Engel, A. (2003) Organization of the G protein-coupled receptors rhodopsin and opsin in native membranes, *J. Biol. Chem. 278*, 21655−21662.
49. Heck, M., Schädel, S. A., Maretzki, D., and Hofmann, K. P. (2003) Secondary binding sites of retinoids in opsin: Characterization and role in regeneration, *Vision Res. 43*, 3003−3010.
50. Schädel, S. A., Heck, M., Maretzki, D., Filipek, S., Teller, D. C., Palczewski, K., and Hofmann, K. P. (2003) Ligand channeling within a G-protein-coupled receptor—The entry and exit of retinals in native opsin, *J. Biol. Chem. 278*, 24896−24903.
51. Okada, T., Fujiyoshi, Y., Silow, M., Navarro, J., Landau, E. M., and Shichida, Y. (2002) Functional role of internal water molecules in rhodopsin revealed by X-ray crystallography, *Proc. Natl. Acad. Sci. U.S.A. 99*, 5982−5987.
52. VanHooser, J. P., Alemán, T. S., He, Y.-G., Cideciyan, A. V., Kuksa, V., Pittler, S. J., Stone, E. M., Jacobson, S. G., and Palczewski, K. (2000) Rapid restoration of visual pigment and function with oral retinoid in a mouse model of childhood blindness, *Proc. Natl. Acad. Sci. U.S.A. 97*, 8623−8628.
53. Noorwez, S. M., Kuksa, V., Imanishi, Y., Zhu, L., Filipek, S., Palczewski, K., and Kaushal, S. (2003) Pharmacological chaperone-mediated *in vivo* folding and stabilization of the P23H-opsin mutant associated with autosomal dominant retinitis pigmentosa, *J. Biol. Chem. 278*, 14442−14450.
54. Spooner, P. J. R., Sharples, J. M., Verhoeven, M. A., Lugtenburg, J., Glaubitz, C., and Watts, A. (2002) Relative orientation between the β-ionone ring and the polyene chain for the chromophore of rhodopsin in native membranes, *Biochemistry 41*, 7549−7555.
55. Das, J., Crouch, R. K., Ma, J.-X., Oprian, D. D., and Kono, M. (2004) Role of the 9-methyl group of retinal in cone visual pigments, *Biochemistry 43*, 5532−5538.
56. Bifone, A., DeGroot, H. J. M., and Buda, F. (1997) Energy storage in the primary photoproduct of vision, *J. Phys. Chem. B 101*, 2954−2958.

BI048404H